The effect of stray grains on the mechanical behavior of nickel-based single crystal superalloy

H.B. Tang, †*H.D. Guo, X.G. Liu, S.H. Yang, L. Huang

Jiangsu Province Key Laboratory of Aerospace Power System, Collaborative Innovation Center for Advanced Aero-Engine, Nanjing University of Aeronautics and Astronautics, Nanjing 210016, China

*Presenting author: ghd@nuaa.edu.cn
†Corresponding author: ghd@nuaa.edu.cn

Abstract

In this paper，a new bicrystal model, consists of primary and stray grains, is proposed to simulate the weakening effect of stray strains generated at geometric discontinuities of single crystal (SC) superalloy. A constitutive model considered crystallographic orientations is introduced, and then the bicrystal model under uniaxial loading is built and analyzed in commercial finite element software ABAQUS. The numerical simulation results indicate that yield strength and elastic modulus of stray grains, which can be determined by the crystallographic orientation, have a significant effect on the deformation of the bicrystal model. To evaluate the local stress rise at the sub-boundary of primary and stray grains, a critical stress based on the yield criterion of SC material is proposed. In the elastic stage, as the elastic modulus difference between primary and stray grains increases, the local stress rise would be more severe. In the elastic-plastic stage II, while the yield strength of primary grains is greater than that of stray grains, the lower the yield strength of stray grains is, the smaller load the bicrystal structure can sustain. Finally an evolution equation of critical stress is constructed with consideration of stray grains under uniaxial loading conditions.

Keywords: Nickel-based single crystal (SC) superalloy, Stray grains, Local stress rise, Critical stress.

1. Introduction

Compared with polycrystalline materials, nickel-based single crystal (SC) superalloy has better mechanical properties at elevated temperature in the absence of weak traditional grain boundaries. During the manufacture of complex structures such as turbine blades, stray grains can be generated in the SC superalloy casting by directional solidification [1-5]. It has been found that thermal condition and mold geometry have a significant impact on the formation of stray grains [5-6]. The disordered temperature distribution at geometric discontinuities, e.g. blade shrouds, turbine blade platforms and turbine blade rabbets, can lead to distortions in the crystal lattice [7]. Usually, stray grains are observed in critical areas with complex stress state, and the mechanical and fatigue characteristics of SC materials can be greatly influenced by stray grains, so the effect of stray grains on SC complex structures should be considered. The basic material properties of SC containing stray grains have been experimentally studied [7, 10-13]. However, there is still a lack of numerical modeling and theoretical analysis of the stray grains effect on SC Materials. In this paper, a SC partition model is built, and the effect of stray grains on the mechanical behaviors of SC materials is further investigated by the bicrystal model through finite element analysis.

2. The SC model considered stray grains

2.1. *The SC partition model*

X-ray topography of SC material Rene N5 containing stray grains were performed by Napolitano et al. [6], and major grain defects were categorized as low-angle boundaries, high-angle boundaries, and spurious grains, shown in Fig. 1(a). The crystal morphology of SC material AM3 containing stray grains was investigated by Zhao et al. [10]. The results showed that stray grains can be divided into several groups by crystallographic orientation, and stray grains in each group were approximately along the same direction. Besides, high-angle boundaries were observed, shown in Fig. 1(b). The casting microstructure of SC material DD6 containing stray grains was studied by Shi et al. [14], and the stray grains along [111] were observed, shown in Fig. 1(c). On the basis of X-ray topography and predictions, the crystallographic orientation and locations of stray grains can be obtained, and then the stray grains can be divided into several partitions. Given a single partition of stray grains, for the case with grains orientated in almost the same direction, it can be still modeled as SC material, and for the case with spurious grains, isotropic model can be used instead.

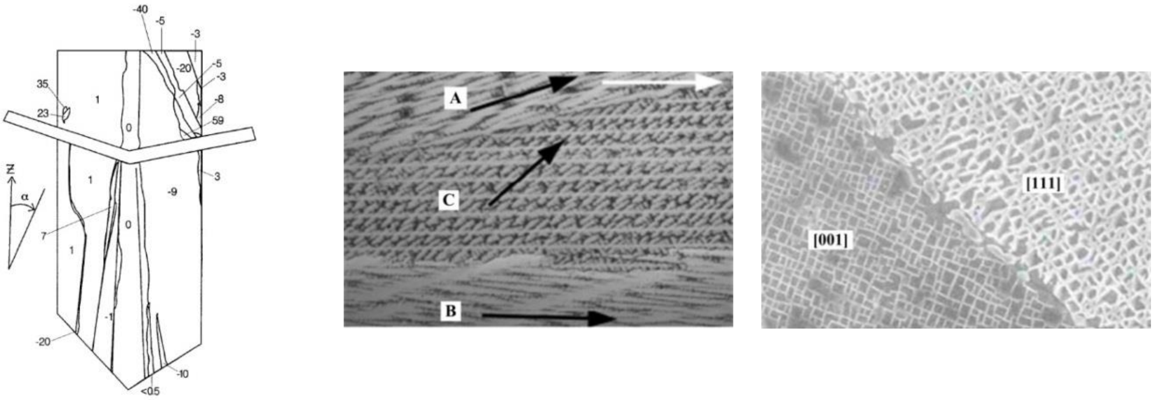

(a) Rene N5 **(b) AM3** **(c) DD6**

Figure 1. SC materials containing stray grains

2.2. *The bicrystal model*

The SC structures containing stray grains will be simplified in the following discussion. Given the crystallographic orientations of primary and stray grains, a bicrystal model containing one group of stray grains is proposed, as detailed in Fig. 2. In Fig.2, the left and right part of the bicrystal model represents the primary and stray grains, respectively. The bicrystal model is fixed at one end and applied with a concentrated load at other end horizontally. β is the angle between the interface of sub-boundary and the orientation of primary grains, and a wide range of β can be expected in the real SC structures.

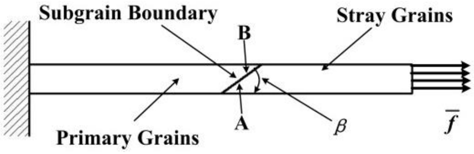

Figure 2. A bicrystal model

3. Material Property Prediction for the bicrystal model

The tensile tests of SC material DD3 along [001], [011] and [111] at 680°C were conducted by Ding [15], and basic material properties are summarized in Table 1. The elastic-plastic parameters of DD3 (ID is QX#.) along each direction, as shown in Table 2, is calculated from the constitutive model given in Appendix A. Since the angle α between crystallographic orientations of primary and stray grains, which is different from β, cannot clearly distinguish the stray grains in different crystallographic orientations, the actual orientation [hkl] is introduced.

Table 1. The tensile test results of DD3 (680 ℃) along [001], [011] and [111]

Temperature (°C)	G (GPa)	μ	$E_{[001]}$ (GPa)
680	113	0.322	129.7
$\phi'_{[001]}$ (GPa)	$\sigma_{y[001]}$ (MPa)	$\sigma_{y[011]}$ (MPa)	$\sigma_{y[111]}$ (MPa)
1.328	943	896	1085

where $\sigma_{y[001]}$, $\sigma_{y[011]}$ and $\sigma_{y[111]}$ are the yield strengths of DD3 along [001], [011] and [111], respectively. $\phi'_{[001]}$ is the plastic modulus of DD3 along [001].

Table 2. Basic material properties of DD3 in selected directions (680 ℃)

ID	Orientation $[hkl]$			α (°)	σ_{ym} (MPa)	E (GPa)	ϕ' (GPa)
	h	k	l				
QX1	0	0.105	1	6	935.50	131.83	1.308
QX2	0	0.177	1	10	924.50	135.65	1.278
QX3	0	0.268	1	15	909.50	143.08	1.237
QX4	0.189	0.189	1	15	911.81	143.35	1.244
QX5	0	0.577	1	30	888.31	180.34	1.183
QX6	0	1	1	45	895.8	207.21	1.204
QX7	0.707	0.707	1	45	1031.18	243.6	1.594
QX8	1	1	1	54.74	1084.8	258.75	1.764

where σ_{ym}, E and ϕ' are the yield strength, elastic modulus and plastic modulus of DD3, respectively.

4. Influence analysis based on the bicrystal model

4.1. *The FE model*

Based on the DD3 bicrystal model as illustrated in Fig. 2, the stress distribution at critical region will be discussed in this section to analyze the effect of stray grains on the mechanical properties of SC material. An 3D model is built in ABAQUS 6.13, and the dimension of the model is $60mm\times10mm\times4mm$, and $\beta=30°$. The primary grains are along [001], and the stray grains are labeled as from QX1 to QX8 for different orientations, as detailed in Table 2. Both primary and stray grains are under axial tension, thus the constitutive relationship of DD3 along corresponding directions should be used. The non-linear large deflection algorithm is enabled through the finite element analysis to accurately capture the local plastic deformation.

4.2. *The critical stress in the bicrystal model*

According to the finite element analysis results, non-uniform stress distribution and the critical region (A or B) can be always observed under axial tensile load. The stress contours obtained from two typical configurations under two different loads are illustrated from Fig. 3(a) to Fig. 3(d).

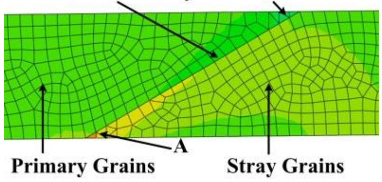

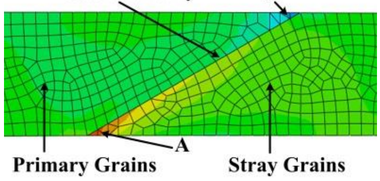

(a) $\overline{f}=765\text{MPa}$ (containing QX5) **(b) $\overline{f}=765\text{MPa}$ (containing QX8)**

(c) $\overline{f}=905\text{MPa}$ (containing QX5) **(d) $\overline{f}=1013\text{MPa}$ (containing QX8)**

Figure 3. Stress contour of the DD3 bicrystal model containing stray grains

where $\overline{f}$ is the applied load.

To evaluate the local stress rise near the sub-boundary, a SC critical stress σ_d is proposed, which can be calculated by Eq. (B.1) from Appendix B. Fig. 4(a) presents the relationship between critical stress σ_d and applied load $\overline{f}$ (nominal surface force) of the DD3 bicrystal model containing stray grains QX5; Fig. 4(b) shows the relationship between σ_d and $\overline{f}$ of the DD3 bicrystal model containing different stray grains (partly). According to Fig. 4(a)-(b), the whole loading process of the model can be divided into three stages:

(1) Elastic stage
(2) Elastic-plastic stage I
(3) Elastic-plastic stage II

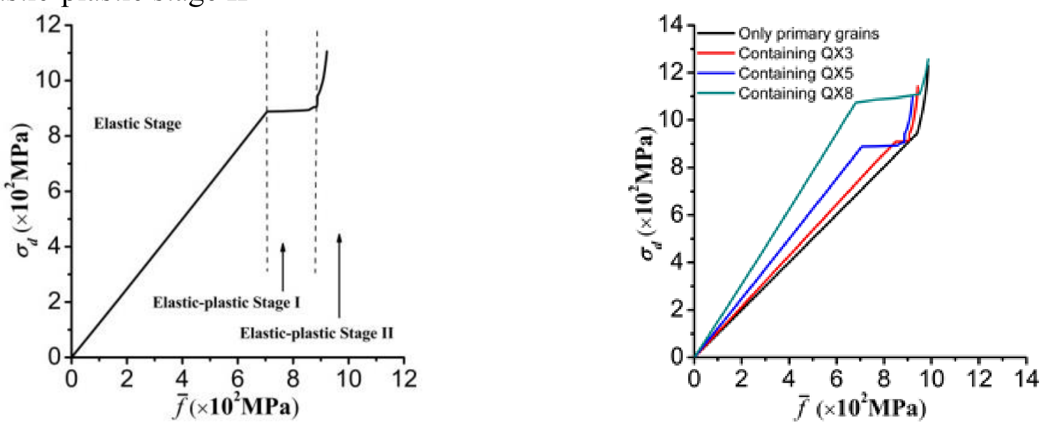

(a) containing QX5 **(b) containing different stray grains**

Figure 4. Relationship between σ_d and $\overline{f}$ of the DD3 bicrystal model

In the elastic stage, the variation of σ_d depends on the elastic modulus of primary grains E_0 and the elastic modulus of stray grains E_{m}. Local high stress is observed obviously near region A, as shown in Fig. 3(a)-(b). As the load increases, the material at region A will yield firstly. In the elastic-plastic stage I, the local stress rise location is still within region A. With the increase of load, the local stress rise tends to less distinct and more stray grains reach the initial yield stress. It could be found that, in the elastic-plastic stage II, the variation of σ_d is mainly determined by the yield strength of primary grains σ_{y0} and the yield strength of stray grains σ_{ym}. While σ_{ym} is smaller than σ_{y0} (e.g. QX5), the critical region will be transferred from A to B, as shown in Fig. 3(c), and with the increase of load, more primary grains reach the initial yield stress; while σ_{ym} is larger than σ_{y0} (e.g. QX8), Region A will always be the most critical location, as shown in Fig. 3(d). By the end of Elastic-plastic stage II, the maximum equivalent stress of the grains with lower yield strength will increase rapidly due to necking, while high stress location around sub-boundary is still a critical region in consideration of the fragility of sub-boundary.

In the elastic stage, as the elastic modulus difference between primary and stray grains increases, the local stress concentration would be more severe. When the grain defect is either a low-angle boundary ($\alpha \leq 15°$) or a high-angle boundary ($\alpha > 15°$), the local stress rise will be unremarkable or significant, respectively. In the Elastic-plastic stage II, while σ_{ym} is smaller than σ_{y0}, the lower σ_{ym} is, the smaller load the bicrystal structure can sustain; while σ_{ym} is greater than σ_{y0}, the maximum load, which the bicrystal structure can sustain, is nearly the same.

4.3. *Evolution equation of the critical stress*

The critical stress observed near the sub-boundary of primary and stray strains has been discussed in previous section, and the evolution equation of the critical stress will be built with considerations of the effect of stray strains.

4.3.1. *Elastic stage*

There is a significant linear correlation between σ_d and $\overline{f}$, as shown in Fig. 4(b). As the slope of the linear relationship k_1 depends on E_0 and E_{m}, $k_1 = 4.57 \times 10^{-6}(E_{\mathrm{m}} - E_0) + 1$ can be calculated by regression analysis. Thus, the evolution equation of σ_d in the elastic stage can be given as,

$$\sigma_d = [4.57 \times 10^{-6}(E_{\mathrm{m}} - E_0) + 1]\overline{f} \tag{1}$$

Since $\sigma_d \leq \min\{\sigma_{\mathrm{y0}}, \sigma_{\mathrm{ym}}\}$, the range of load can be obtained in Eq. (2).

$$0 \leq \overline{f} \leq \frac{\min\{\sigma_{y0}, \sigma_{\mathrm{ym}}\}}{4.57 \times 10^{-6}(E_{\mathrm{m}} - E_0) + 1} \tag{2}$$

4.3.2. *Elastic-plastic stage I*

The range of load can be expressed as,

$$\frac{\min\{\sigma_{\mathrm{y0}}, \sigma_{\mathrm{ym}}\}}{4.57 \times 10^{-6}(E_{\mathrm{m}} - E_0) + 1} < \overline{f} < \min\{\sigma_{\mathrm{y0}}, \sigma_{\mathrm{ym}}\} \tag{3}$$

With increase of applied load, σ_d is nearly the same, as detailed in Fig. 4(b). Thus, the evolution equation of σ_d in this stage has the following form,

$$\sigma_d = \sigma_{\mathrm{ym}} \tag{4}$$

4.3.3. *Elastic-plastic stage II*

The range of load can be written as,

$$\overline{f} > \min(\sigma_{y0}, \sigma_{ym}) \tag{5}$$

In the DD3 bicrystal model, the difference in the magnitudes of E_0 and E_m will result in a different critical region, and σ_d will change in a different way, too. Fig. 5(a)-(b) present the relationship between σ_d and $\overline{f}$ of the DD3 bicrystal model containing different stray grains in the elastic-plastic stage II.

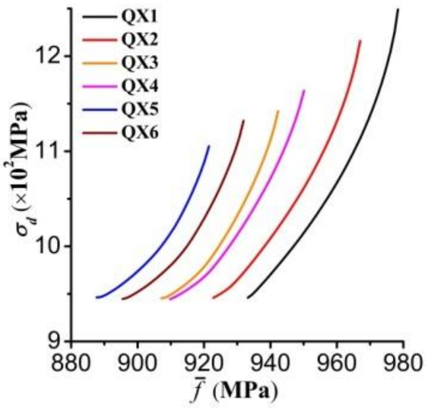

（a） $\sigma_{ym} < \sigma_{y0}$

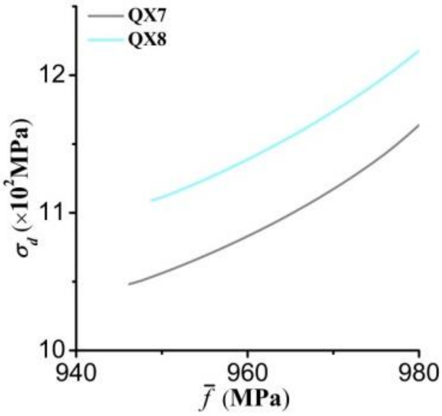

（b） $\sigma_{ym} > \sigma_{y0}$

Figure 5. Relationship between σ_d and $\overline{f}$ of the DD3 bicrystal model containing different stray grains in the elastic-plastic stage II

While $\sigma_{ym} < \sigma_{y0}$, the evolution equation of σ_d in this stage has the following form:

$$\sigma_d = 0.9(\overline{f} - \sigma_{ym})^{1.49} + \sigma_{y0} \tag{6}$$

While $\sigma_{ym} > \sigma_{y0}$, the evolution equation of σ_d in this stage has the following expression:

$$\sigma_d = 1.55(\overline{f} - \sigma_{y0})^{1.23} + \sigma_{ym} \tag{7}$$

Finally, the evolution equation of σ_d is summarized by Eq. (8).

$$\sigma_d = \begin{cases} [4.57\times10^{-6}(E_0 - E_m)+1]\overline{f}, & 0 \le \overline{f} \le \dfrac{\min\{\sigma_{y0}, \sigma_{ym}\}}{4.57\times10^{-6}(E_0 - E_m)+1} \\ \sigma_{ym}, & \dfrac{\min\{\sigma_{y0}, \sigma_{ym}\}}{4.57\times10^{-6}(E_m - E_0)+1} < \overline{f} < \min\{\sigma_{y0}, \sigma_{ym}\} \\ 0.9(\overline{f} - \sigma_{ym})^{1.49} + \sigma_{y0}, & \overline{f} > \min\{\sigma_{y0}, \sigma_{ym}\} \text{ and } \sigma_{ym} < \sigma_{y0} \\ 1.55(\overline{f} - \sigma_{y0})^{1.23} + \sigma_{ym}, & \overline{f} > \min\{\sigma_{y0}, \sigma_{ym}\} \text{ and } \sigma_{ym} > \sigma_{y0} \end{cases} \tag{8}$$

When $\sigma_{ym} < \sigma_{y0}$ and $\overline{f}$ is nearby σ_{ym}, the critical region will be transferred and σ_d will increase dramatically, which is not included in Eq. (8).

4.4. *Influence analysis of the angle between sub-boundary and orientation of primary grains*

The effect of β on SC material containing stray grains is also analyzed by the model shown in Fig 2. The primary grains are along [001], and the stray grains are QX5. β equals to $20°$, $30°$ and $45°$, respectively. Fig. 6 presents the relationship between σ_d and $\overline{f}$ of the DD3 bicrystal model with different β. The result shows that the local stress rise will be more distinct in elastic stage and the loading process will be longer, with decrease of β. However, β has little influence on mechanical behavior of SC material containing stray grains in the elastic-plastic stage II.

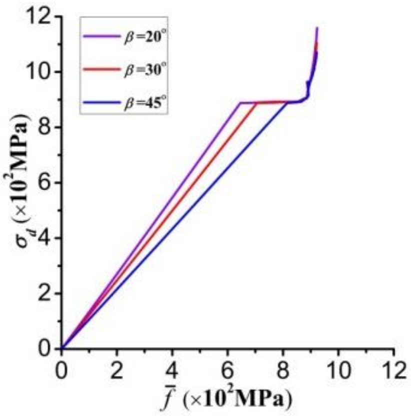

Figure 6. Relationship between σ_d and $\overline{f}$ of the DD3 bicrystal model with different β

5. Discussions

1. The proposed SC partition model can be used to simulate the SC materials containing several groups of stray grains. The local high stress can be found near the sub-boundary of primary and stray grains. The local stress distribution and critical stress will also be influenced by the geometry of SC structure.
2. As the applied load increases, the local high stress region is always observed near the sub-boundary. Given the fragility of sub-boundary, the effect of stray grains should be considered in the analysis of the mechanical behavior and fatigue characteristics of SC complex structures.

6. Conclusions

In this paper，a new bicrystal model, consists of primary and stray grains, is proposed to simulate the weakening effect of stray strains generated at geometric discontinuities of SC material. A constitutive model considered crystallographic orientations is introduced, and then the bicrystal model under uniaxial loading is built and analyzed. The numerical simulation results indicate that yield strength and elastic modulus of stray grains, which can be determined by the crystallographic orientation, have a significant effect on the deformation of the bicrystal model. To evaluate the local stress rise at the sub-boundary of primary and stray grains, a critical stress based on the yield criterion of single crystal material is proposed. In the elastic stage, as the elastic modulus difference between primary and stray grains increases, the local stress rise would be more severe. In the elastic-plastic stage II, while the yield strength of primary grains is greater than that of stray grains, the lower the yield strength of stray grains is, the smaller load the bicrystal structure can sustain. Hence, the effect of stray grains on the mechanical and fatigue characteristics of SC complex structures should not be neglected. Finally an evolution equation of critical stress is constructed with consideration of stray grains under uniaxial loading conditions.

Appendix A. Constitutive model of SC superalloy

T-G criterion [16] can be used to describe the yield behavior of SC superalloy:

$$Y^2 = [(P_1 + P_2)^2 + P_6]^{\frac{1}{2}} \tag{A.1}$$

$$P_1 = \frac{A_1}{6}(S_{ii} - S_{jj})^2; P_2 = B_1 S_{ij}^2; P_6 = C_1[(S_{kk} - S_{jj})^2 + (S_{kk} - S_{ii})^2]S_{ij}^2$$

Based on Drucker postulation and associated flow rule [17], T-G criterion can be used as plastic potential. The constitutive model of SC superalloy can be constructed by isotropic hardening model. As $\bar{\sigma} = Y$, plastic potential has the following form:

$$U = \bar{\sigma}^2 \tag{A.2}$$

Since isotropic hardening model is adopted, hardening parameter is given as,

$$\mathrm{K} = \bar{\varepsilon}_p \tag{A.3}$$

Hence, the elasto-plastic matrix can be finally derived as,

$$[C]_{ep} = [C]_e - \frac{[C]_e \left\{\frac{\partial \bar{\sigma}}{\partial \sigma}\right\} \left\{\frac{\partial \bar{\sigma}}{\partial \sigma}\right\}^{\mathrm{T}} [C]_e}{\mathrm{H}' + \left\{\frac{\partial \bar{\sigma}}{\partial \sigma}\right\}^{\mathrm{T}} [C]_e \left\{\frac{\partial \bar{\sigma}}{\partial \sigma}\right\}} \tag{A.4}$$

Appendix B. Critical stress of SC superalloy

According to the yield criterion of SC superalloy presented in Appendix A, stress of the critical region can be constructed as,

$$\bar{\sigma} = [(P_1 + P_2)^2 + P_6]^{\frac{1}{4}} \tag{B.1}$$

Reference

[1] Zhang, X. L., Zhou, Y. Z., Jin, T. and Sun, X. F. (2012) Study on the tendency of stray grain formation of Ni-based single crystal superalloys, *Acta Metallurgica Sinica* **48**, 1229-1236.

[2] Li, B., Zhu, S. Z., Li, X. and Pan, G. Z. (2012) Research on gating system of a directional solidified blade, *Foundry* **61**, 81-83.

[3] Xuan, W. D., Ren, Z. M., Ren, W. L., Yu, J. B. and Chen, C. (2011) Effect of seed crystal orientation on the stray grain of directional solidified Ni-based superalloy, *Journal of Iron and Steel Research* **23**, 368-372.

[4] D'Souza, N., Jennings, P. A., Yang, X. L., Dong, H. B., Lee, P. D. and Mclean, M. (2005b) Seeding of single-crystal superalloys role of constitutional undercooling and primary dendrite orientation on stray-grain nucleation and growth, *Metallurgical and materials transactions* **36**, 657-666.

[5] Yang, X. L., Dong, H. B., Wang, W. and Lee, P. D. (2004a) Microscale simulation of stray grain formation in investment cast turbine blades, *Materials Science and Engineering* **396**,129-139.
[6] Napolitano, R.E., Schaefer, R. J. (2000) The convergence-fault mechanism for low-angle boundary formation in single-crystal castings, *Journal of Materials Science* **35**, 1641-1659.
[7] Yan, X. J., Deng, Y., Sun, R. J. and Xie, J. W. (2011) Study of fatigue property variation at different regions on a DS turbine blade, *Acta Aeronautica et Astronautica Sinica* **32**, 1930-1936.
[8] A. de Bussac, C. A. Gandin. (1997a) Prediction of a process window for the investment casting of dendritic single crystals, *Materials Science and Engineering* **237**, 35-42.
[9] Zhao, X. B., Liu, L., Zhang, W. G., Qu, M., Zhang, J. and Fu, H. Z. (2011) Analysis of competitive growth mechanism of stray grains of single crystal superalloys during directional solidification process, *Rare Metal Materials and Engineering* **40**, 9-13.
[10] Zhao, J. Q., Li, J. R., Liu, S. Z. and Yuan, H. L. (2008) Effects of low angle grain boundaries on tensile properties of single crystal superalloy DD6, *Journal of Materials Engineering* **8**, 73-76.
[11] Shi, Z. X., Li, J. R., Liu, S. Z. and Zhao, J. Q. (2009) Tensile properties of twist low angle boundary of DD 6 single crystal superalloy, *Journal of Aeronautical Materials* **6**, 88-92
[12] Shi, Z. X., Li, J. R., Liu, S. Z. and Zhao, J. Q. (2012) Effect of LAB on the stress rupture properties and fracture characteristic of DD6 single crystal superalloy, *Rare Metal Materials and Engineering* **41**, 962-966.
[13] Shi, Z. X., Liu, S. Z., Zhao, J. Q. and Li, J. R. (2015) Effect of low angle boundary on high cycle fatigue properties of single crystal superalloy, *Transactions of materials and heat treatment* **6**, 52-57.
[14] Shi, Z. X., Liu, S. Z., Li, J. R. (2015) Study on the stray grain microstructure of DD6 single crystal superalloy, *Foundry* **64**, 153-156.
[15] Ding, Z. P. (2005) *Study on multiaxial low cycle fatigue damage of single crystal nickel-based superalloy*, Central South University.
[16] Tang, H. B. (2014) *Effect of geometric discontinuities on the fatigue behavior of single crystal superalloy,* Nanjing University of Aeronautics and Astronautics.
[17] Shi, F. (2012) *Re-development of ANSYS and application examples*, China Water & Power Press, Beijing.